

Dopamine encoding of novelty facilitates efficient uncertainty-driven exploration

Yuhao Wang¹, Armin Lak², Sanjay G. Manohar³, and Rafal Bogacz¹

¹MRC Brain Network Dynamics Unit, University of Oxford, Oxford, UK

²Department of Physiology, Anatomy and Genetics, University of Oxford, Oxford, UK

³Nuffield Department of Clinical Neurosciences, University of Oxford, Oxford, UK

September 15, 2023

Short title: Uncertainty-driven exploration in the basal ganglia

Abstract

When facing an unfamiliar environment, animals need to explore to gain new knowledge about which actions provide reward, but also put the newly acquired knowledge to use as quickly as possible. Optimal reinforcement learning strategies should therefore assess the uncertainties of these action-reward associations and utilise them to inform decision making. We propose a novel model whereby direct and indirect striatal pathways act together to estimate both the mean and variance of reward distributions, and mesolimbic dopaminergic neurons provide transient novelty signals, facilitating effective uncertainty-driven exploration. We utilised electrophysiological recording data to verify our model of the basal ganglia, and we fitted exploration strategies derived from the model to data from behavioural experiments. We also compared the performance of directed exploration strategies inspired by our basal ganglia model with classic variants of upper confidence bound (UCB) strategy in simulation. The exploration strategies inspired by the basal ganglia model performed better than the classic algorithms in simulation in some cases, and we found qualitatively similar results in fitting model to behavioural data compared with the fitting of more idealised normative models with less implementation level detail. Overall, our results suggest that transient dopamine levels in the basal ganglia that encode novelty could contribute to an uncertainty representation which efficiently drives exploration in reinforcement learning.

26 Author summary

27 Humans and other animals learn from rewards and losses resulting from their actions to maximise their
28 chances of survival. In many cases, a trial-and-error process is necessary to determine the most rewarding
29 action in a certain context. During this process, determining how much resource should be allocated
30 to acquiring information (“exploration”) and how much should be allocated to utilising the existing
31 information to maximise reward (“exploitation”) is key to the overall effectiveness, i.e., the maximisation
32 of total reward obtained with a certain amount of effort. We propose a theory whereby an area within the
33 mammalian brain called the basal ganglia integrates current knowledge about the mean reward, reward
34 uncertainty and novelty of an action in order to implement an algorithm which optimally allocates
35 resources between exploration and exploitation. We verify our theory using behavioural experiments and
36 electrophysiological recording, and show in simulations that the model also achieves good performance
37 in comparison with established benchmark algorithms.

38 1 Introduction

39 In order to survive, animals must develop efficient strategies of reinforcement learning to maximise the
40 reward of their actions. An important factor in effective reinforcement learning is optimised modulation
41 of exploration and exploitation. If an animal already possesses knowledge about a safe and nutritious
42 food source, say a fruit, should it prioritise seeking for that familiar fruit in future foraging, or should it
43 keep trying out unfamiliar alternatives?

44 In this study, we generalise from real-world scenarios and define exploration to be any behaviour by
45 a learning agent that favours actions which are sub-optimal in terms of their expected rewards accord-
46 ing to the current best knowledge, and exploitation as behaviour that chooses the optimal action with
47 highest expected reward. Modulating exploration and exploitation is no trivial task, not least because in
48 real-world scenarios there are often factors such as motivation [1], non-stationarity of the environment [2]
49 and balancing of short-term and long-term reward optimisation [3] that together influence the optimal
50 strategy in complex ways. Here, we focus on a quintessential problem without the additional complex-
51 ity to establish a feasible neural mechanism for exploration-exploitation modulation based on reward
52 uncertainty estimation.

53 The problem in question is the classic multi-armed bandit task [4, 5, 6, 7]. By design of the task,
54 rewards are simplified to one-dimensional numerical values and actions to having no difference in effort
55 exertion – these simplifications also effectively eliminate the necessity to consider the contribution of sen-
56 sorimotor error to uncertainty. During the task, the agent has to choose one out of multiple slot machines
57 (“arms of the bandit”) to play from on each trial. Each of the arms produces a reward represented as a
58 scalar numerical value sampled when played. The rewards from each arm are sampled from a probability

59 distribution associated with the arm, which remains stationary throughout each block of trials. The
60 agent is made aware of the start and end of each block of trials as well as the length of each block, and
61 is instructed to maximise the total reward received within each block.

62 In the context of this task, if an agent follows a greedy strategy [8] that does not involve any exploration
63 at all and always prefers the optimal action according to current knowledge, they would simply play each
64 arm exactly once at the beginning of each block of trials and proceed to always choose the one that returns
65 the highest reward in the one trial for the rest of the block. The performance of this simple strategy
66 quickly deteriorates as the spreads of the reward distributions get larger. A simple modification of the
67 greedy strategy, often dubbed the ε -greedy strategy [8], adds unmodulated exploration. On each trial,
68 there is a probability of $1 - \varepsilon$ that the agent chooses the empirically optimal action, and a probability of
69 ε that the agent explores by randomly choosing among the actions with equal probability. We call this
70 unmodulated exploration since the chances of an exploratory choice of action is constant and therefore
71 independent of the level of uncertainty the agent experiences. Such unmodulated exploratory behaviour
72 already improves the robustness of the strategy significantly, but lacks in adaptability.

73 Finding an optimal strategy for the multi-armed bandit with modulated exploration has been an
74 ongoing quest in the world of statistics since Robbins [9] first mentioned it in the context of sequential
75 analysis, and studies such as Lai and Robbins [10], Katehakis and Robbins [11] and Auer et al. [6]
76 discussed optimal strategies that achieve the theoretical asymptotic performance bound [10] under certain
77 constraints. These strategies belong to a class called the upper confidence bound (UCB) algorithm, which
78 computes an uncertainty bonus for each action that modulates exploration. This falls under the category
79 of directed exploration strategies that Gershman [12] discussed in comparison with random exploration
80 strategies. A hybrid strategy combining features of directed and random exploration was also proposed
81 and mathematically specified, and these three qualitatively different types of exploration strategies were
82 fitted to human behavioural data from a two-armed bandit experiment [12]. Results show that the
83 hybrid strategy explains human behaviour significantly better. In this work, we take inspiration from
84 the normative modelling of behaviour in Gershman [12] and propose a novel model of the basal ganglia
85 which facilitates similar exploration strategies, thus attempt to bridge the gap between algorithmic level
86 study of behaviour and neural implementation.

87 The novel basal ganglia model is based on a series of studies started by Mikhael and Bogacz [13], who
88 proposed that the direct pathway with D1 receptor-expressing neurons and the indirect pathway with
89 D2 receptor-expressing neurons in the striatum can together achieve learning of both expectation and
90 variability of the reward resulting from an action during reinforcement learning. Based on this assumption,
91 tonic dopamine level in the striatum can influence the overall level of risk seeking in behaviour because
92 of the opposite effects dopamine has on D1 and D2 neurons. Specifically, higher dopamine level should
93 result in a stronger preference for more risky actions with more variable outcomes. Mikhael and Bogacz

94 [13] reviewed experimental evidence consistent with this prediction. In this work, we further consider
95 the effect of fast transient changes in dopamine level on decision making. Specifically, we note that the
96 transient activity of dopaminergic neurons can encode novelty [14, 15, 16, 17, 18, 19], and show that
97 with the novelty signal provided by dopamine, the basal ganglia circuit modelled can facilitate efficient
98 uncertainty-driven exploration strategies.

99 Later in this section, we introduce the example task used throughout this study and review the
100 normative behavioural models of exploration from Gershman [12] in more detail. We also review a model
101 of the basal ganglia learning reward uncertainty Mikhael and Bogacz [13]. In **Results**, we first show
102 that an extended version of this model can approximate the normative exploration strategies. Next, we
103 compare electrophysiologically recorded activities of dopaminergic neurons in the ventral tegmental area
104 to the form of novelty signal required for efficient exploration according to our model. We then make
105 adjustments to the model to more accurately reflect experimental results, and compare the resulting
106 exploration strategies with the normative strategies in Gershman [12] when fitted to human behaviour
107 in a bandit task. We also compare the performance of a strategy derived from the basal ganglia model
108 with that of UCB strategies in Auer et al. [6] in a simulated bandit task. In **Discussion**, we compare
109 our model with several other theories [16, 20, 21] on the role of dopaminergic neurons in exploration
110 modulation, and formalise experimental predictions and future directions.

111 1.1 The multi-armed bandit task

112 Before introducing reinforcement learning models with uncertainty-driven exploration, we formalise here
113 the nomenclature associated with the multi-armed bandit problem used as the example task throughout
114 this work. On each of the τ sequential trials (indexed $t \in \{1, 2, \dots, \tau\}$) within a block, the agent needs
115 to choose one from a total of K available slot machines (“arms” of the bandit, indexed $i \in \{1, 2, \dots, K\}$)
116 to play. The chosen arm on each trial is denoted $c[t] \in \{1, 2, \dots, K\}$. After the selection is made on each
117 trial, a reward of a certain numerical value is randomly sampled from the reward distribution associated
118 with the selected arm (denoted R_i) and presented to the agent.

119 1.2 Normative strategies of uncertainty-driven exploration

120 The following strategies for uncertainty-driven exploration all rely on dynamically updated estimates of
121 mean rewards from each arm, which we denote $Q_i[t]$ for arm i at trial t , as well as associated posterior
122 uncertainty levels about the mean estimates, which we denote $\sigma_i[t]$. A conceptually straightforward
123 approach to modelling the updating of these latent variables is with Kalman filtering [12], although the
124 neural implementation of such algorithm is potentially complex [22, 23].

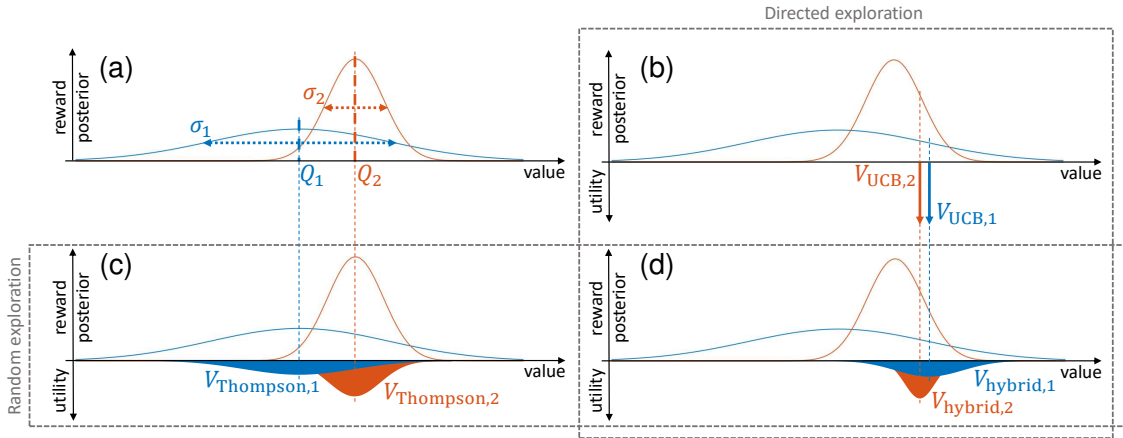


Figure 1. Demonstration of different types of exploration strategies. The distributions on the upward axis in each panel represent the (Gaussian) posterior estimations of the mean rewards from two arms. The distributions on the downward axes in panels (b)(c)(d) are example distributions of different types of value utility functions (without noise). (a): Q_1 and Q_2 are posterior means and σ_1 and σ_2 are posterior standard deviations, representations of posterior uncertainty levels. (b): with a directed exploration strategy such as UCB, the value utilities (Equation 1) are deterministically biased from the posterior means by an amount proportional to the posterior standard deviation. (c): with a random exploration strategy such as Thompson sampling (in the two-arm case), the value utilities (Equation 4) are sampled around the posterior means with spreads proportional to the posterior standard deviations, so the posterior standard deviations do not bias the action selection, but only modulate the stochasticity. (d): with a hybrid exploration strategy, the value utilities (Equation 27) are sampled around the deterministically biased values of the directed strategy and with spreads proportional to the posterior standard deviations as in the random strategy.

125 **1.2.1 Directed exploration: upper confidence bound (UCB)**

126 With estimations of reward expectation and uncertainty levels for each arm of the bandit learned, the
127 upper confidence bound strategy uses the value utility variable [12]

128
$$V_{UCB,i}[t] = Q_i[t] + \theta\sigma_i[t] + eZ \quad (1)$$

129 associated with each arm to make the selection at each trial (Figure 1(b)). Here θ and e are weighting
130 parameters and $Z \sim \mathcal{N}(0, 1)$ is a standard Gaussian random variable. The arm with the greatest observed
131 value utility is chosen on each trial. The sum of the first two terms gives the upper bound of a confidence
132 interval for the mean reward estimation (hence “upper confidence bound”) and the third term introduces
133 unmodulated stochasticity, which can be considered as accounting for system noise. Parameter θ controls
134 the weighting of the “uncertainty bonus”, or equivalently the confidence level of the confidence interval.
135 The larger its value, the more optimistic and exploratory the strategy is. In the two-armed case ($K =$
136 2, $i \in \{1, 2\}$), the probability of choosing arm 1 over 2 is

137
$$p(c[t] = 1) = p(V_{UCB,1}[t] > V_{UCB,2}[t]) \quad (2)$$

138
$$= \Phi \left(\frac{Q_1[t] - Q_2[t] + \theta(\sigma_1[t] - \sigma_2[t])}{\sqrt{2e^2}} \right), \quad (3)$$

140 where $\Phi(\cdot)$ denotes the cumulative density function of the standard Gaussian distribution. This choice
141 probability is dependent on the difference in mean reward estimations and the difference in uncertainty
142 levels (“relative uncertainty” in Gershman [12]). Under this strategy, an action currently believed to
143 be less rewarding can actually be the favoured option in terms of choice probability. This is a defining
144 characteristic of a directed exploration strategy, and it generalises to bandit tasks with more than two
145 arms.

146 **1.2.2 Random exploration: Thompson sampling**

147 A different exploration strategy named Thompson sampling [24, 12, 25, 3, 26] can be achieved by defining
148 a different value utility (Figure 1(c))

$$149 \quad V_{\text{Thompson},i}[t] = Q_i[t] + \gamma\sigma_i[t]Z. \quad (4)$$

150 Instead of using the uncertainty level as a deterministic bonus, Thompson sampling samples from a
151 posterior distribution defined by the estimated mean and uncertainty. The specific formalisation here
152 assumes a Gaussian posterior of the form $\mathcal{N}(Q_i[t], \gamma\sigma_i[t])$. Similar to θ in Equation 1, the parameter γ
153 controls the weighting of uncertainty levels by scaling the standard deviation of the Gaussian posterior.
154 In the two-armed ($K = 2$) case, the probability of choosing arm 1 over 2 under Thompson sampling is
155 then

$$156 \quad p(c[t] = 1) = p(V_{\text{Thompson},1}[t] > V_{\text{Thompson},2}[t]) \quad (5)$$

$$157 \quad = \Phi \left(\frac{Q_1[t] - Q_2[t]}{\sqrt{\gamma^2(\sigma_1^2[t] + \sigma_2^2[t])}} \right). \quad (6)$$

159 This probability is again dependent on the difference in mean reward estimations, and also dependent on
160 the sum in uncertainty levels rather than the difference. Thus, the action with higher estimated mean
161 reward is always favoured in terms of choice probability. This is the defining characteristic of random
162 exploration strategies [12]. However, when Thompson sampling is applied to a bandit task with more
163 than two arms, this property does not generalise¹, and therefore Thompson sampling is not strictly a
164 random exploration strategy in this more general case.

165 **1.2.3 Hybrid exploration strategy**

166 Using regression analysis and model fitting on behavioural data, Wilson et al. [3] and Gershman [12] have
167 shown that humans employ an uncertainty-driven strategy that shows characteristics of both directed

¹When there are more than two arms, the ranking of all the arms by choice probability is not necessarily the same as the ranking by mean estimations, unlike in the two-arm case.

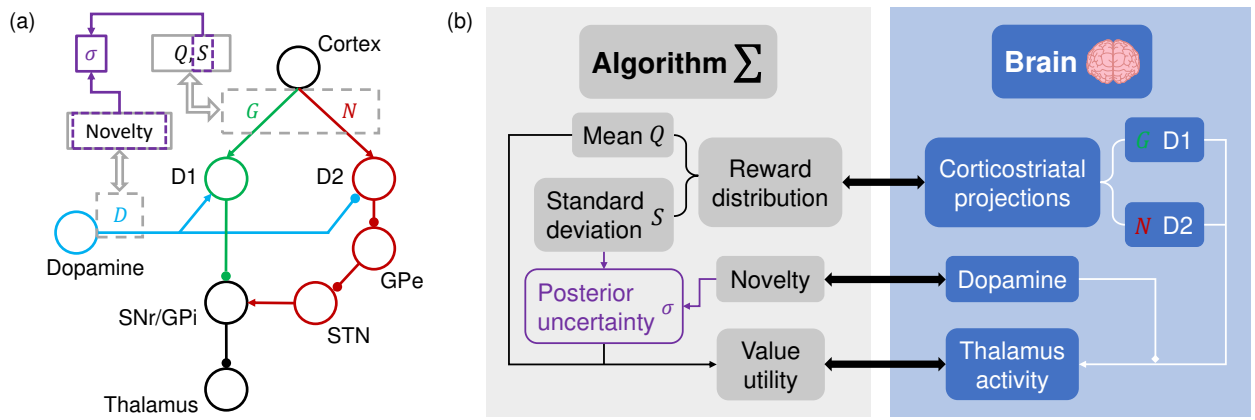


Figure 2. Illustration of the basal ganglia model. (a): circuit diagram representing the basal ganglia, adapted from Möller and Bogacz [1]. D1/D2 receptor-expressing neurons are involved in direct and indirect striatal pathways, respectively, and dopamine has opposite effects on the two pathways. Both pathways project to the thalamus. (b): mapping of learned latent parameters in the proposed algorithm (left) onto neural metrics (right).

168 and random exploration during the bandit task. Gershman [12] used the choice probability

$$169 \quad p(c[t] = 1) = \Phi \left(\gamma \frac{Q_1[t] - Q_2[t]}{\sqrt{\sigma_1^2[t] + \sigma_2^2[t]}} + \theta(\sigma_1[t] - \sigma_2[t]) \right), \quad (7)$$

170 to represent such a hybrid strategy. Here, a change in either total uncertainty or relative uncertainty
 171 independent of the other can influence action selection through either the sum of uncertainty levels on
 172 the denominator or the difference of uncertainty levels on the numerator, respectively. Note that this
 173 choice probability cannot be derived from explicit value utility variables (analogous to those given by
 174 Equations 1 and 4, Figure 1(d)) associated with each of the arms.

175 **1.3 The basal ganglia model**

176 These normative strategies presented above have so far not been connected to biological implementations.
 177 In this study, we show that basal ganglia circuits could potentially support a mechanism for both belief
 178 updating and producing value utilities for action selection. We first briefly review a previously described
 179 model, and in Results we show the necessary extensions to allow exploration strategies.

180 **1.3.1 Learning the mean and spread of reward distribution**

181 Mikhael and Bogacz [13] first proposed that, by utilising both direct and indirect striatal pathways that
 182 include D1 and D2 receptor-expressing neurons respectively, mean and spread (specifically the mean
 183 deviation) of the reward distribution associated with a certain action can be learned simultaneously
 184 in the basal ganglia. According to the model, the neural circuit containing both pathways (Figure 2)
 185 takes an input representing an available action at the current state from the cortex. The direct pathway

186 with D1 neurons has an excitatory effect on the thalamus, while the indirect pathway with D2 neurons
 187 has an inhibitory effect. The combined effects of both pathways in the thalamus represent the current
 188 value utility of the action. In a task involving action selection, multiple parallel circuits are required to
 189 represent all available actions. The model assumes that belief updating or learning occurs in the weights
 190 of corticostriatal projections. We denote the weights of projections from the cortex to the D1 neurons in
 191 the direct striatal pathway and D2 neurons in the indirect pathway $G_i[t]$ (G for “GO”) and $N_i[t]$ (N for
 192 “NO-GO”), respectively, based on the effects of the two pathways on the thalamus. Subscript i indicates
 193 the action (choice of arm in the bandit task) being encoded, and t denotes the trial number within a
 194 block of trials, as in the previous section.

195 Learning rules in this circuit have been extensively discussed previously [13, 1, 27]. One basic version
 196 can be written as

$$197 \quad \delta[t] = R_{c[t]} - \frac{1}{2}(G_{c[t]}[t] - N_{c[t]}[t]), \quad (8)$$

$$198 \quad G_{c[t]}[t+1] = G_{c[t]}[t] + \alpha_{c[t]}[t]f_\epsilon(\delta[t]) - \beta G_{c[t]}[t], \quad (9)$$

$$199 \quad N_{c[t]}[t+1] = N_{c[t]}[t] + \alpha_{c[t]}[t]f_\epsilon(-\delta[t]) - \beta N_{c[t]}[t], \quad (10)$$

200 where $f_\epsilon(x) = x$ for $x > 0$ and $f_\epsilon(x) = \epsilon x$ for $x < 0$ ($0 < \epsilon < 1$). $\delta[t]$ gives the reward prediction
 201 error at each trial, as will be shown later. The piecewise linear activation function $f_\epsilon(\cdot)$ over the reward
 202 prediction error is an essential element of this learning rule, and evidence shows dopaminergic neurons
 203 encoding reward prediction error do exhibit this type of modulation in their responses [28]. The decay
 204 terms with scaling parameter β keeps the learning variables bounded. Following this learning rule, G_i is
 205 a “satisfaction learning” reinforced by better-than-expected outcomes and to a lesser extent diminished
 206 by worse-than-expected outcomes, while N_i is a “disappointment learning” reinforced by worse-than-
 207 expected outcomes and to a lesser extent diminished by better-than-expected outcomes. $\alpha_i[t]$ is the
 208 learning rate parameter taking values in $(0, 1)$ for all values of i and t . The substitutions
 209

$$210 \quad Q_i[t] = (G_i[t] - N_i[t])/2, \quad (11)$$

$$211 \quad S_i[t] = (G_i[t] + N_i[t])/2 \quad (12)$$

212 transform the learning rule in Equations 9 and 10 into

$$214 \quad Q_{c[t]}[t+1] = Q_{c[t]}[t] + \alpha_{c[t],q}[t]\delta[t] - \beta Q_{c[t]}[t], \quad (13)$$

$$215 \quad S_{c[t]}[t+1] = S_{c[t]}[t] + \alpha_{c[t],s}[t]|\delta[t]| - \beta S_{c[t]}[t], \quad (14)$$

216 where $\alpha_{i,q}[t] = \alpha_i[t](1 + \epsilon)/2$ and $\alpha_{i,s}[t] = \alpha_i[t](1 - \epsilon)/2$.

218 Further idealisation of this learning rule gives

219
$$\delta[t] = R_{c[t]} - Q_{c[t]}[t], \quad (15)$$

220
$$Q_{c[t]}[t+1] = Q_{c[t]}[t] + \alpha_{c[t],q}[t]\delta[t], \quad (16)$$

221
$$S_{c[t]}[t+1] = S_{c[t]}[t] + \alpha_{c[t],s}[t](|\delta[t]| - S_{c[t]}[t]) \quad (17)$$

223 as seen in Moeller et al. [27], with the constraint $\alpha_{i,q}[t] > \alpha_{i,s}[t]$. Here, we simply set these to be constant
224 values across the experiments for each agent, so that

225
$$\alpha_{i,q}[t] = \alpha_q, \quad (18)$$

226
$$\alpha_{i,s}[t] = \alpha_s. \quad (19)$$

228 Under this learning rule, Q_i and S_i converge to the stationary point

229
$$Q_i^* = \mathbb{E}\{R_i\}, \quad (20)$$

230
$$S_i^* = \mathbb{E}\{|R_i - \mathbb{E}\{R_i\}|\}, \quad (21)$$

232 which is to say that, at the stationary point, Q_i and S_i are the mean reward and mean deviation of
233 reward for arm i , respectively. Without using the idealisation, the stationary point is different, but
234 with appropriate parameters still a good representation of mean and spread of the reward distribution
235 albeit with some additional scaling and bias [13]. Another variation of the learning rule that achieves
236 the exact stationary point given in Equations 20 and 21 has also been proposed [23], but for the purpose
237 of this study, we are satisfied with using the idealised learning rule given in Equations 15 to 17. The
238 $Q_i[t]$ variable, like that in the normative strategies, is a dynamically updated estimation of the mean
239 reward. The exact dynamics of this variable in the two implementations is different, since the normative
240 strategies update using Kalman filtering, and the basal ganglia model uses the learning rule derived from
241 the dynamics of direct and indirect pathways. The $S_i[t]$ variable fundamentally differs from $\sigma_i[t]$ in the
242 normative strategies, as it is only an estimation of the spread of reward distribution, whereas $\sigma_i[t]$ is the
243 posterior standard deviation of the mean estimation from Kalman filtering which eventually diminishes
244 with repeated observations. We show later how the basal ganglia model might produce an equivalent
245 $\sigma_i[t]$ variable and use it to inform action selection.

246 **1.3.2 Effect of dopamine**

247 Dopamine was found to have opposite modulating effects on the excitability of D1 and D2 neurons [29],
248 increasing that of D1 neurons and reducing that of D2 neurons (Figure 2). Denoting the dopamine level
249 in the striatum as $D_i[t]$, we can thus express the thalamus activity as a result of the activities of the two

250 pathways using

$$251 \quad T_i[t] = \left(\frac{1 + \lambda D_i[t]}{2} \right) G_i[t] - \left(\frac{1 - \lambda D_i[t]}{2} \right) N_i[t] + eZ, \quad (22)$$

252 where λ is a scaling factor that reflects the strength of dopaminergic modulation. The model assumes
 253 here that dopamine level in the circuit has the same modulating effect on the two pathways. $T_i[t]$ is used
 254 as the value utility for action selection, much like $V_{UCB,i}[t]$ and $V_{Thompson,i}[t]$ in the normative strategies.
 255 Despite this relationship, we will keep using $T_i[t]$ to denote the value utilities derived from the basal
 256 ganglia model that can be directly mapped to activity in the thalamus. $G_i[t]$ and $N_i[t]$ in Equation 22
 257 follow the learning rule given above, and eZ is a noise term accounting for all sources of random noise
 258 within the circuit. Substituting $G_i[t]$ and $N_i[t]$ with $Q_i[t]$ and $S_i[t]$, Equation 22 is equivalent to

$$259 \quad T_i[t] = Q_i[t] + \lambda D_i[t] S_i[t] + eZ. \quad (23)$$

260 From Equation 23, it is easy to arrive at the experimental prediction that elevated tonic dopamine level
 261 in the striatum should lead to higher level of risk seeking in behaviour, and evidence in support of this
 262 prediction has been reviewed [13].

263 2 Results

264 2.1 Dopamine encoding novelty leads to effective exploration

265 Following the reinforcement learning and action selection rules from Equations 15 to 23, if dopamine level
 266 in the basal ganglia circuit stays constant from trial to trial during action selection, actions with higher
 267 estimated mean reward (more rewarding on average) and greater reward spread (more risky) are always
 268 favoured. This has certain benefits in exploration modulation, especially at the early stages of exposure
 269 to a new environment (e.g. at the beginning of a new block of trials in the bandit task).

270 We now know from previous studies discussed earlier that the posterior uncertainty of mean estimation
 271 is the more effective modulator for exploration. In other words, we need a representation of the $\sigma_i[t]$
 272 variable in the basal ganglia circuit as in the normative strategies. Once again, the learned variables $Q_i[t]$
 273 and $S_i[t]$ according to Equations 15 to 17 are estimators of the mean and mean deviation of a reward
 274 distribution. The updates for a certain arm happen only when that arm is chosen and consequently the
 275 reward from it observed during a trial. Therefore, the number of times arm i has been chosen up until
 276 trial t , denoted $n_i[t]$, is the sample size from which these estimations are made. Following the central
 277 limit theorem and with a neutral prior on the mean reward, we can represent the posterior uncertainty
 278 on mean estimation using

$$279 \quad \sigma_i[t] = \frac{S_i[t]}{\sqrt{n_i[t]}}. \quad (24)$$

280 Since both $Q_i[t]$ and $S_i[t]$ are dynamically updated, and at the stationary point $S_i[t]$ gives the absolute
 281 mean deviation rather than standard deviation, $\sigma_i[t]$ is a biased approximation of the posterior standard
 282 deviation unlike the equivalent value obtained through Kalman filtering in the normative strategies.

283 It is evident now that, in order for the basal ganglia circuit modelled to compute posterior uncertainty,
 284 a signal correlated to the sample size $n_i[t]$ is necessary. This is where we formally look at the trial-by-trial
 285 variations of dopamine level. While more commonly associated with reward prediction error, transient
 286 dopamine activities have also been found to be correlated to novelty in certain reinforcement tasks [15,
 287 16]. Since novelty naturally has negative correlation with the sample size, we make the assumption about
 288 the specific form of dopamine level with

$$289 \quad D_i[t] = (\eta Z + \nu) \frac{1}{\sqrt{n_i[t]}} \quad (25)$$

290 or equivalently

$$291 \quad D_i[t] \sim \mathcal{N} \left(\frac{\nu}{\sqrt{n_i[t]}}, \frac{\eta^2}{n_i[t]} \right), \quad (26)$$

292 which is a noisy representation with both mean level and variability negatively correlated to the sample
 293 size. Substituting this into Equation 23 gives

$$294 \quad T_i[t] = Q_i[t] + \lambda(\eta Z + \nu)\sigma_i[t] + eZ. \quad (27)$$

295 This represents an effective value utility ($V_{\text{hybrid},i}$ in Figure 1(d)). In the two-armed case, it leads to the
 296 choice probability

$$297 \quad p(c[t] = 1) = p(T_1[t] > T_2[t]) \quad (28)$$

$$298 \quad = \Phi \left(\frac{Q_1[t] - Q_2[t] + \lambda\nu(\sigma_1[t] - \sigma_2[t])}{\sqrt{\lambda^2\eta^2(\sigma_1^2[t] + \sigma_2^2[t]) + 2e^2}} \right). \quad (29)$$

300 The exploration strategy this basal ganglia model produces shares the same essential property of the
 301 hybrid strategy given earlier by Equation 7, in that both the relative uncertainty and total uncertainty
 302 levels affect the choice probability. This model also has isolated UCB and Thompson sampling strategies
 303 nested in, which can be recovered when either η or ν is zero.

304 We have thus shown that an extension of an existing biological model of the basal ganglia yields
 305 an exploration strategy with important similarities to efficient normative strategies, that qualitatively
 306 matches past experiments.

307 In the rest of **Results**, we demonstrate the merits of the extended model of the basal ganglia from
 308 three perspectives. First, we verify the assumption made in extending the model about the specific
 309 mathematical form of the response of dopamine level to novelty using electrophysiological recording data.

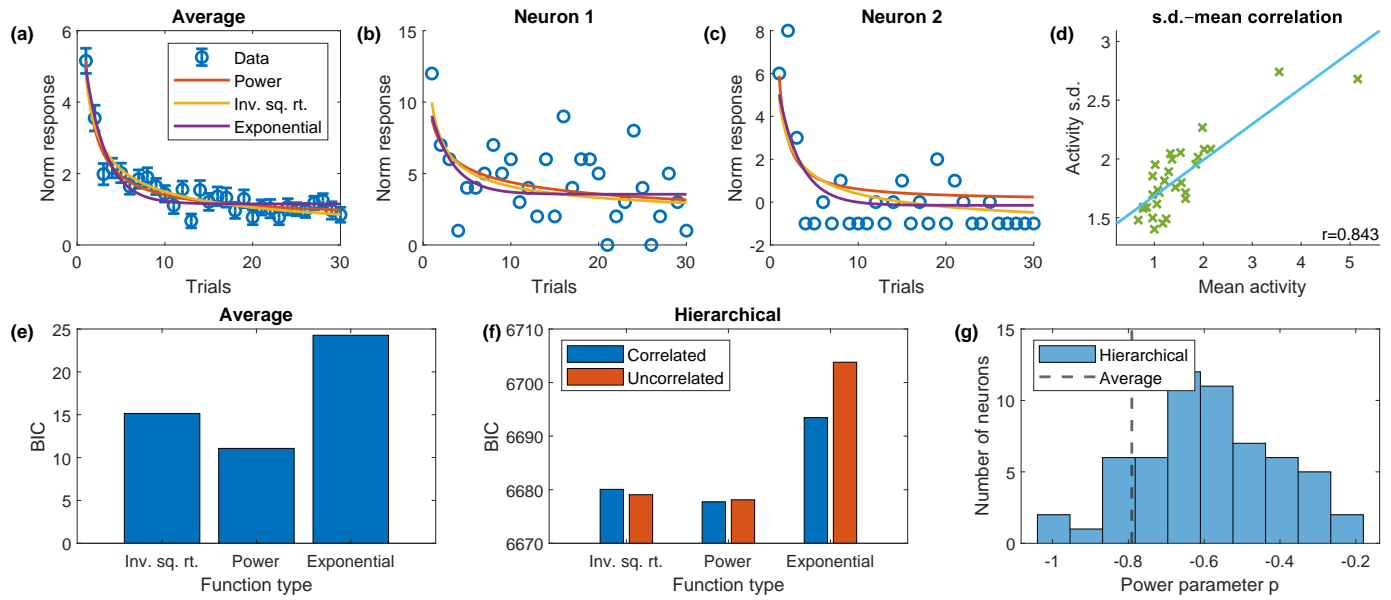


Figure 3. Results from function fitting to recording data collected during the early phase of the response of VTA dopamine neurons to stimuli during Pavlovian learning. (a): experimental data points of average activity and standard error overlaid with best fitting curves of three different function forms (power function, inverse square root function i.e. power function with power parameter fixed at -0.5 , exponential function). (b)(c): experimental data points of the activity of two example neurons overlaid with best fitting curves of the same three function forms obtained through hierarchical model fitting. (d): scatter plot of standard deviation of activity against average activity at each trial overlaid with best fitting straight line (correlation $r = 0.843$). (e): Bayesian information criterion (BIC) values for the fitting of functions to average activity data, showing that the power function is the best fitting. (f): BIC values for fitting hierarchical models (with correlated and uncorrelated model parameters) to individual neurons' recording data, again showing the power function is the best fitting. (g): power parameter p obtained through fitting to average activity and hierarchical model fitting (shown as a histogram).

310 Next, we compare the fitting to human behavioural data of the exploration strategies from the model
 311 with that of the normative strategies. Finally, we show the performance of the basal ganglia strategy in
 312 more difficult tasks in comparison with classic UCB strategies.

313 2.2 Modelling of dopaminergic novelty response

314 In Equations 25, it is assumed that the dopamine level is inversely proportional to the square root of
 315 the number of observations of outcomes from an arm. We seek experimental evidence that supports this
 316 assumption on the specific mathematical form of dopaminergic response to novelty.

317 Lak et al. [14] studied the response of dopaminergic neurons to conditioned stimuli during the Pavlo-
 318 vian learning task using electrophysiological recording in awake behaving monkeys. During the experi-
 319 ment, novel reward-predicting visual stimuli, which the animals have never seen before, were presented
 320 to animals. Different stimuli were associated with one of three (25%, 50% or 75%) probabilities of re-
 321 ward (a drop of juice). Neural data were collected during the learning task using extracellular single-cell
 322 recording of 58 neurons in the ventral tegmental area (VTA) identified as dopaminergic neurons using

323 established criteria. These neurons likely projected to the ventral striatum where D1 and D2 neurons are
324 found [30, 31]. It was shown that the response of the dopaminergic neurons was divided into two distinct
325 temporal phases. The firing rates during the late phase 0.2 to 0.6 s after cue onset differentiated reward
326 probabilities predicted by different stimuli in learned animals. This response pattern is consistent with
327 the theory that dopamine signals reward prediction error. The firing rates during the early phase 0.1 to
328 0.2 s after cue onset were independent of reward probabilities associated with the cue throughout the
329 experiment even after learning was completed, but decreased as the stimuli causing the response were
330 repeatedly presented, thus reflected stimulus novelty [14]. We focus on the early phase novelty signal
331 here to investigate whether its quantitative form resembles the normatively ideal form given earlier in
332 Equations 25 and 26.

333 We performed function fitting on the trial-by-trial evolution of normalised and baseline-subtracted
334 firing rates of dopaminergic neurons during the novelty response phase (Figure 3). The fitting was done
335 using both the average activity of the 58 recorded neurons (Figure 3(a)), and using individual neuron data
336 with a hierarchical model (Figure 3(b)(c)). The functions and fitting methods used are described in more
337 detail in **Methods**. Results from both hierarchical model fitting and fitting to average activity suggest
338 that the inverse square root function (the closest to the normatively ideal form) fits better than the
339 exponential function, but the best fitting function is the power function with three function parameters
340 (Figure 3(e)(f)). For fitting using the average activity, the best fitting function is therefore of the form

$$341 \quad \bar{D}_i[t] = \mathbb{E}\{D_i[t]\} = m + kn_i^\pi[t], \quad (30)$$

342 and the best fitting power parameter π is -0.791 to three s.f., which differs significantly from -0.5 which
343 gives the inverse square root function ($p < 0.05$, two-tailed t -test). Also differing from the ideal form is
344 the non-zero intercept m ($p < 0.05$, two-tailed t -test). In further analysis, we focus on the fitting using
345 average activity. This allows us to analyse the relationship between novelty and variability of the neuronal
346 responses – the normative analysis (Equations 24 to 29) show that there should also be positive correlation
347 between novelty and neuronal response variability. Specifically, we assume that the relationship between
348 standard deviation of activities and the number of observations takes identical form as the mean activity.
349 We therefore performed linear regression analysis on the mean and standard deviation of activities from
350 the 58 recorded neurons (Figure 3(d)), and found a strong relationship ($r = 0.843$ to three s.f., $p < 10^{-8}$,
351 two-tailed t -test). This relationship can be expressed as

$$352 \quad \text{s.d.}(D_i[t]) = \sqrt{\mathbb{E}\{(D_i[t] - \mathbb{E}\{D_i[t]\})^2\}} = a + b\bar{D}_i[t]. \quad (31)$$

353 One difference we found between the best fitting function to experimental data and the normatively ideal
354 form is again the non-zero ($p < 10^{-18}$) intercept a in Equation 31.

355 2.3 Model refinement based on dopamine data

356 We can now make some amendments to the extensions on the basal ganglia model, utilising the form of
357 dopaminergic novelty response derived from electrophysiological recording data given in Equations 30 and 31.
358 The modified expression for dopamine level is

$$359 \quad D_i[t] = (a + b\bar{D}_i[t])Z + \bar{D}_i[t] \quad (32)$$

$$360 \quad = (a + bm + bkn_i^\pi[t])Z + m + kn_i^\pi[t], \quad (33)$$

362 or equivalently

$$363 \quad D_i[t] \sim \mathcal{N} \left(m + kn_i^\pi[t], (a + b(m + kn_i^\pi[t]))^2 \right). \quad (34)$$

364 To summarise, this experimentally determined expression of dopaminergic activity is different from the
365 ideal form given in Equations 25 and 26 in that it has the general power function in place of the inverse
366 square root function, and it also has additional constant terms in both the deterministic (mean) and
367 stochastic (standard deviation) components. This leads to an alternative form of posterior uncertainty
368 level (modified from Equation 24)

$$369 \quad \hat{\sigma}_i[t] = S_i[t]n_i^\pi[t], \quad (35)$$

370 which then leads to the output to the thalamus (analogous to the ideal version given in Equation 27) to
371 take the form

$$372 \quad T_i[t] = Q_i[t] + \lambda (((a + bm)Z + m)S_i[t] + (bkZ + k)\hat{\sigma}_i[t]) + eZ. \quad (36)$$

373 Compared to the ideal form, there remains a term with $S_i[t]$ which is the result of the constant parameters
374 m and a in the fitted functions in Equations 30 and 31.

375 2.4 Model fitting to behavioural experiment data

376 We have previously drawn comparison in multiple occasions between the exploration strategies derived
377 from the basal ganglia model and the normative strategies from Gershman [12]. While these share
378 common characteristics in their algorithms, we also highlighted some important differences, most notably
379 in the learning rules and the resulting representation of posterior uncertainty. Gershman [12] designed a
380 two-armed bandit task and performed behavioural experiment involving human participants, and fitted
381 the normative strategies to the behaviour of the participants during the task. It was discovered that the
382 hybrid strategy fitted the data better than isolated directed or random exploration strategies. In this
383 study, we fitted strategies from the basal ganglia model (with parameters describing dopamine novelty
384 response fixed to values estimated above from the activity of dopaminergic neurons) to the same data for
385 an algorithmic level comparison of the strategies. For completeness, we fitted not only the general hybrid

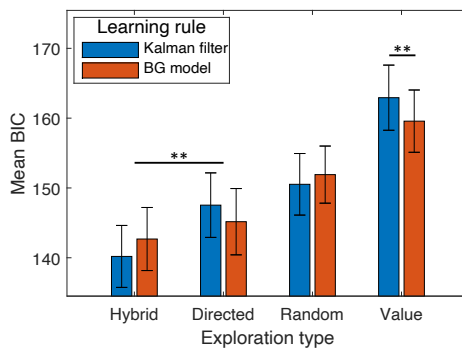


Figure 4. Mean of BIC values from trial-by-trial model fitting to behaviour of individual participants in a two-armed bandit task. The reinforcement learning models fitted employ two different learning rules (Kalman filtering as in Gershman [12] and basal ganglia derived learning rule (see **Methods** for details). Four models with each learning rule were fitted, each with a different exploration strategy. Following each of the two learning rules, the model with hybrid exploration strategy is the best fitting.

386 strategy defined by Equation 36, but also the special directed and random exploration only strategies.

387 During the experiment of Gershman [12], participants faced blocks of ten trials during which the
 388 rewards from two arms were drawn from fixed Gaussian distributions with different means but identical
 389 variances. The participants were instructed to maximise the total reward over each block (length known).
 390 It is worth highlighting at this point that all of the strategies fitted to this dataset are based on the
 391 fundamental assumption that the exploration strategy used by the agent remains stationary on a trial-
 392 by-trial basis, i.e. the strategy is indifferent to the number of trials remaining. This assumption is mostly
 393 valid for this experimental setup.

394 Trial-by-trial fitting with stochastic maximum likelihood methods was used to obtain optimal param-
 395 eters of the basal ganglia strategies for each individual participant. Once the optimal parameters were
 396 obtained, the corresponding maximum likelihoods were further converted into Bayesian information crite-
 397 rion (BIC) statistics used for comparison. This offsets the potential benefits brought by extra parameters
 398 with a penalty. The strategies fitted to behaviour and methods for fitting are described in more detail in
 399 **Methods**.

400 Figure 4 shows comparison of BIC values from fitting two sets of strategies with different learning
 401 rules – one with Kalman filtering as the learning rule from Gershman [12], and the other derived from the
 402 novel basal ganglia model, with fixed reinforcement learning rates defined in Equations 18 and 19. Each
 403 set consists of four variations with different types of uncertainty-driven exploration (or lack thereof) –
 404 the hybrid exploration strategy, the directed and random exploration only strategies, and a “value-only”
 405 strategy that does not use any modulated exploration (equivalent to standard Rescorla–Wagner learning
 406 for the basal ganglia strategies). There is no significant difference in the goodness of fit between models
 407 with same exploration strategies but different learning rules (except for the value-only models, $p < 0.01$,
 408 two-tailed t -test). Among models with the same learning rule, the model with hybrid exploration strategy
 409 is significantly better fitting than others ($p < 0.01$, two-tailed t -test). We have thus confirmed the key

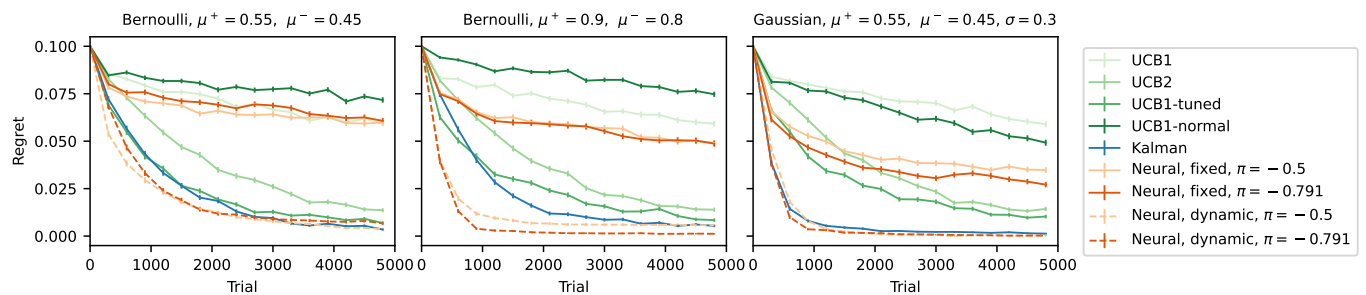


Figure 5. Performance comparison of neural UCB strategies inspired by the basal ganglia model against other UCB algorithms in different bandit tasks. Per-trial regret (defined as the difference between the expected reward of the optimal action and the expected reward of the chosen action at each trial) is plotted against trial number in each panel. Error bars show standard errors over $N = 1000$ repeated simulations. Panel titles describe the tasks – each task had one arm with mean reward μ^+ and nine arms with mean reward μ^- . For the Gaussian task, all arms have the same standard deviation $\sigma = 0.3$. We tested neural UCB strategies with two different values of power parameter π which are the ideal value predicted by the model (-0.5) and the value that best describes neural recording data (-0.791). Both fixed learning rate (solid lines) and dynamic (decaying) learning rate (dashed lines) versions of the neural UCB strategies were tested.

410 finding of Gershman [12] that humans use a hybrid strategy of directed and random exploration in bandit
 411 tasks using a more mechanistic modelling framework based on physiology. Our results also show that
 412 the exploration strategies derived from the basal ganglia model are similar to the normative strategies
 413 with Kalman filtering in terms of their abilities to interpret behaviour at the algorithmic level. Given the
 414 more idealised learning rule used in the normative strategies that does not account for potential individual
 415 differences across participants, one would perhaps expect significantly better fitting from the basal ganglia
 416 strategies. However, since BIC is a metric that penalises larger numbers of model parameters, a potential
 417 explanation could be that the effect of individual differences in this task is relatively small, so that
 418 the decrease in BIC from better fitting is outweighed by the increase from additional penalty for extra
 419 parameters.

420 2.5 Performance in simulation of bandit tasks

421 Variations of UCB strategies have been extensively investigated in analytical studies to assess their
 422 performances in multi-armed bandit tasks [10, 11, 6]. We compared the performance of UCB strategies
 423 that use the learning rule and value utility based on the basal ganglia model with several other efficient
 424 UCB variations [6, 12] in simulation. More details about the models used can be found in **Methods**.

425 The simulated multi-armed bandit tasks all involve ten arms, with the reward from each arm drawn
 426 from distributions of the same form. Nine of these ten reward distributions in each task were identical,
 427 with the other having a slightly higher mean reward. Due to the difficulty of these tasks, a large number of
 428 trials were simulated for each experiment. We follow the convention used by Auer et al. [6] and define the
 429 regret at each trial as the difference between the mean reward of the most rewarding action and the mean
 430 reward of the chosen action on that trial. Figure 5 shows the results from simulations of three different

431 tasks. For each task, regret is plotted over trial number for each strategy. The first two tasks were two
432 cases of the Bernoulli bandit with the same difference in mean reward between optimal and sub-optimal
433 actions, and the third was a Gaussian bandit task with the same mean rewards as the first Bernoulli task
434 but smaller reward variances. We were able to reproduce the qualitative findings from Auer et al. [6]
435 regarding the classic UCB strategies: the more complex UCB2 and UCB1-tuned perform better than UCB1
436 in all experiments; UCB1-normal (which is a variation of UCB1 optimised for Gaussian bandits) performs
437 better than standard UCB1 only in the Gaussian task – despite the Gaussian task being less demanding
438 than the Bernoulli task with the same mean rewards due to smaller reward variances, all strategies from
439 Auer et al. [6] except UCB1-normal performed worse in the Gaussian task. The Kalman filter strategy from
440 Gershman [12] consistently outperform all the classic strategies. It is also able to take advantage of the
441 smaller reward variances in the Gaussian task, and therefore has the most significant advantage against
442 the other strategies in this task. The neural strategies with fixed learning rates (Equations 18 and 19)
443 have worse performance than the Kalman filter strategy and the best performing strategies from Auer
444 et al. [6]. Following this observation, we experimented with variations of the neural strategies with
445 dynamically adjusted learning rates defined by

$$446 \quad \alpha_{i,q}[t] = \alpha_{0,q} \frac{m + kn_i^\pi[t]}{m + k}, \quad (37)$$

$$447 \quad \alpha_{i,s}[t] = \alpha_{0,s} \frac{m + kn_i^\pi[t]}{m + k}, \quad (38)$$

449 which gradually reduce the rate of updating mean reward and reward variability estimations as learning
450 progresses, and result in significantly improved performance over the fixed learning rate strategies in
451 all tasks. The improved performance of the neural strategies overall exceeds that of the Kalman filter
452 strategy. Note that in fitting the different models to human behaviour, we did not observe a significant
453 difference between the fixed learning rate neural models and the Kalman filter model unlike in these
454 simulations. This is likely due to the behavioural experiments involving much shorter blocks of trials
455 compared with the simulations.

456 We also discovered in analysing neural recording data that the representation of novelty by dopaminer-
457 gic neurons does not necessarily follow the ideal form the normative model predicts. Here we see that the
458 difference in the specific representation of novelty (i.e. the difference in the value of the power parameter
459 π) has little effect on the performance of the resulting exploration strategies in simulations.

460 Overall, the results of the simulations suggest that a strategy based on the basal ganglia model can
461 perform better than the classic UCB strategies and the Kalman filter UCB strategy in a range of bandit
462 tasks, given that the learning rate is dynamically adjusted and decays with novelty. However, fixed
463 learning rate strategies do not perform nearly as well.

464 3 Discussion

465 Our results suggest that the fast transient variations of dopaminergic neuron activity can encode novelty
466 in a way that could contribute to representation of posterior uncertainty in the basal ganglia during rein-
467forcement learning. The uncertainty representation could then be used to facilitate exploration strategies
468 that perform well in simulation and are similar to a normatively ideal construction. In this section, we
469 further discuss the implications of the results and new experimental predictions that can be derived from
470 the model, as well as potential future directions.

471 3.1 Functions of dopamine in reinforcement learning

472 The quantitative analysis on the novelty response of dopaminergic neurons made possible by high resolu-
473 tion recording is fundamental to all results from this study. The role of dopamine has always been central
474 in efforts of understanding reinforcement learning. In particular, the transient activity of dopaminergic
475 neurons is widely considered to encode reward prediction errors [32, 15] used to update the predictions
476 of action outcomes. This theory is supported by a plethora of experimental evidence. In fact, the exper-
477 imental results [14] we analysed also provide support for this theory. The activity of VTA dopaminergic
478 neurons recorded from 0.2 to 0.6 s after cue onset as well as their responses to rewards are highly con-
479 sistent with the pattern predicted by the reward prediction error theory [14]. Saliently for this work,
480 there has also been observations of correlation between activity of dopaminergic neurons and novelty [16,
481 15]. This additional variability is often treated as being multiplexed into the reward prediction error
482 signals as a bonus component. Experimental results from Lak et al. [14] provide an alternative view on
483 the multiple factors correlated with transient activity of dopaminergic neurons by observing the different
484 response patterns during the temporal window 0.1 to 0.2 s after cue versus the later 0.2 to 0.6 s window.
485 This suggests the possibility that the novelty and reward prediction error signals are carried by the same
486 dopaminergic neurons yet can still be fully decoupled. Based on this hypothesis, we constructed our rein-
487forcement learning model of the basal ganglia that uses the reward prediction error in belief updates and
488 uses the novelty signal combined with other learned latent variables to modulate exploration in decision
489 making, which is fundamentally different from the “novelty as a bonus” view in many previous models
490 [16]. The dual function of fast transient dopamine variations is also supported by evidence uncovered
491 more recently that dopamine conveys motivational value on short timescales and that there exist possible
492 mechanisms for the same target neurons of dopamine to switch between different interpretation modes
493 [33].

494 We found from simulations of challenging multi-armed bandit tasks that learning rates dynamically
495 adjusted according to novelty level can have significant performance benefits. Naturally, this leads to the
496 speculation that the novelty signal delivered by dopaminergic neurons can also modulate the plasticity

497 of corticostriatal connections. Some recent experiments suggest that this mechanism could in fact exist
498 in the brain [34, 35]. From the data used in this study, one could theoretically find conjectural evidence
499 for or against the hypothesis, e.g. by investigating whether the outcome of an “explore” trial (a trial
500 on which the option with lower Q value is chosen, likely to be associated with higher novelty signal) is
501 statistically more influential on the outcome of the next trial (suggesting a higher learning rate). Within
502 the model framework of reinforcement learning through direct and indirect striatal pathways, Möller
503 et al. [23] had a different take on modulated belief updating, which considers the circuit dynamics at the
504 time of reward presentation and predicts that the reward prediction error itself should be scaled by the
505 estimated spread of the reward distribution (Equation 12). Theoretically, this could be combined with
506 the learning rate modulation by novelty, and from a physiological perspective, the novelty signal should
507 take effect on the target striatal neurons before reward presentation, whereas the dynamics that leads to
508 the scaled prediction error signal occurs after reward presentation.

509 While the analysis in this work is centred around the transient changes in dopamine level, the tonic
510 dopamine level in the striatum could also influence the circuit dynamics and consequently reinforcement
511 learning behaviour. According to our model, the most significant effect of higher tonic dopamine level
512 should be an overall higher level of risk preference, and consequently a stronger effect of relative un-
513 certainty on directed exploration. Mikhael and Bogacz [13] reviewed experimental evidence in support
514 of this prediction, and Costa et al. [17] demonstrated that elevated tonic dopamine level resulted in in-
515 creased novelty seeking, which can be interpreted as a form of uncertainty preference. However, a more
516 up to date literature contains interesting experimental results that are not necessarily consistent with
517 this prediction. For example, [36] found that stronger striatal dopamine transmission reduced the effect
518 of relative uncertainty on directed exploration.

519 There are also several studies suggesting that high level of tonic dopamine reduces random exploration.
520 Cieślak et al. [37] discovered that genetic disruption of glutamate receptors in dopaminergic and D1
521 neurons (which reduced dopamine transmission) lead to overall more stochastic and less reward-driven
522 choices, while Adams et al. [38] found similar effects of reduced D2 receptor occupancy (which also
523 indicated reduced dopamine transmission). Cinotti et al. [39] also found similar results through the use
524 of dopamine receptor antagonist. However, it is worth emphasising that our model makes prediction
525 on the effects of dopamine on directed exploration, rather than random exploration, and the opposite
526 effects of tonic dopamine level on these two types of exploration may suggest they rely on fundamentally
527 different mechanisms.

528 This literature of experimental work highlights the overall complex nature of the influence of tonic
529 dopamine level on reinforcement learning. In this work, we used normalised firing rate data which
530 themselves does not contain any information about the tonic baseline. Correspondingly, our model of the
531 basal ganglia does not explicitly account for the effect of tonic dopamine levels, but the different resulting

532 model parameters across individual participants from fitting model to behavioural data could potentially
533 be correlated to this.

534 We used electrophysiological recording data obtained during a Pavlovian conditioning task to study the
535 novelty response of dopaminergic neurons [14]. In this context, novelty is naturally associated with each
536 cue presented in the experiment since there was no action required, whereas the model we are proposing
537 handles reinforcement learning tasks with action selections, and includes a novelty value assigned to each
538 action. In fact, within the same study, Lak et al. [14] also recorded during a two-armed bandit task in
539 which one familiar cue and one novel cue (and actions associated with each) were present. The recorded
540 dopaminergic neurons showed response to the number of times the novel action was selected that is highly
541 similar to the cue novelty response in the conditioning task, therefore suggesting that the recorded VTA
542 dopaminergic neurons could also encode action novelty during learning.

543 3.2 Alternative theories of exploration modulation in the brain

544 The model we propose in this work suggests that the basal ganglia are responsible for both learning
545 the associations of high-level actions with resulting rewards and using this information to select actions
546 following near-optimal strategies. A related model from Humphries et al. [20] also highlights the role of
547 the basal ganglia in decision making while describing the relevant circuit dynamics in more detail. These
548 authors made experimental predictions about the effect of tonic dopamine level on the level of random
549 exploration, which suggest that an increase in dopamine level should generally lead to more exploitative
550 behaviour. This qualitatively differs from what our model would suggest, and is supported by some but
551 not all related experimental evidence as discussed in the previous section. Jaskir and Frank [21] proposed
552 another model of exploration modulation in the basal ganglia, which includes a description of the trial-
553 by-trial variation of dopamine level at action selection. Instead of a simple novelty signal, these authors
554 proposed a “meta-critic” mechanism that learns the overall reward level of the entire environment and
555 controls the dopamine level at action selection accordingly. This results in more exploratory behaviour in
556 overall “richer” environments. This meta-critic also operates on a longer timescale compared to the type
557 of dopaminergic dynamics in the model we propose in this study. The authors also compared *in silico*
558 performance comparison which put their model ahead of classic UCB strategies. However, this model
559 is only defined for Bernoulli bandit tasks that produced binary reward outcomes in experiments and
560 simulations. The mean reward and reward standard deviation following a Bernoulli reward distribution
561 are always correlated, and it is not trivial what effect this feature had on the conclusion reached by the
562 authors. A continuous reward distribution is a more realistic representation of real-world scenarios, and
563 we have shown in this work that the exploration strategy based on our basal ganglia model can effectively
564 modulate exploration and exploitation in a bandit task with continuous (Gaussian) reward distribution.

565 Our analysis of the novelty response of dopaminergic neurons suggests that the way novelty is encoded

566 in dopamine level could be the source of a hybrid strategy of directed and random exploration. Given
567 that this type of strategy is prominent in behaviours, there have also been prior studies looking for
568 the underlying mechanism in the brain. Some of these studies found significant correlations between
569 exploratory behaviour and activities in certain cortical regions, and specifically found cortical regions
570 that are linked with only one of directed or random exploration but not the other [40, 41]. These theories
571 on the role of the cortex in exploration are mostly beyond the field of view of this study, but it is of course
572 entirely plausible that the basal ganglia are not the sole source of control over exploration modulation.

573 3.3 Experimental predictions and future directions

574 From a higher level perspective, the ideal follow-up to this work would involve an integrated experimental
575 design with suitable cognitive task and capability to manipulate and monitor dopamine level or activity
576 level of dopaminergic neurons in the relevant brain areas. To begin with, purely regarding the task
577 design, the setup of Gershman [12] is not the most suitable for a study comparing the fitting of different
578 strategies. Longer trial blocks with more challenging tasks would be better for distinguishing the learning
579 rules, and having different reward variances both for different options in the same block and from block to
580 block would provide more informative data and also prevent the subjects forming a prior on the variances
581 over multiple blocks. A task design with both the mean rewards and reward variances for each option
582 randomly chosen for each block of trials would theoretically be the best at revealing the learning dynamics
583 at the algorithmic level.

584 At the implementation level, the most interesting next step would be to directly verify the role of
585 transient variations in dopamine level in exploration modulation. This would need to involve manipulation
586 of the activity of dopaminergic neurons with high temporal precision relative to option presentation
587 during a multi-armed bandit task. Specifically, manually inducing a short temporal period of high
588 dopamine release in the striatum right after presentation of options (within 0.2 s) should lead to higher
589 tendency of exploration (risk seeking) in the action selection that immediately follows. Since this action
590 selection occurs before any belief update can happen, any such effect can only be the result of exploration
591 modulation but not learning. Conversely, inhibition of dopaminergic signals within the same temporal
592 window should lead to stronger exploitative tendency in the following action selection. The strength of
593 the effect of this manipulation should also vary with the spread of the reward distribution, since this is
594 combined with the novelty signal to produce the posterior uncertainty according to our model.

595 For the basal ganglia to facilitate a hybrid exploration strategy, the variability of the transient novelty
596 response of dopaminergic neurons as well as the mean response needs to be modulated (Equation 34).
597 The source of this variability is currently ambiguous. The mechanism most consistent with the model
598 would involve a large number of dopaminergic neurons projecting to each striatal neuron, and only one
599 or a few taking effect on any given trial. This does not seem very realistic, and yet another unlikely

600 requirement of this setup is that somehow the relevant D1 and D2 striatal neurons encoding for the
601 same option need to read out from the same dopaminergic neurons on each trial. A somewhat more
602 likely assumption is that the trial-by-trial variability of the same dopaminergic neurons projecting to each
603 striatal neuron facilitates the sampling. This also does not require the unrealistic assumption that related
604 D1 and D2 neurons always selectively receive from the same dopaminergic neurons, but still requires the
605 dopaminergic neurons projecting to them to have the same upstream source, which is nevertheless much
606 more reasonable. Given the large differences in functions fitted to individual neurons even when using
607 normalised firing rates (Figure 3(b)(c)), it is tricky to build a completely rigorous model based on this
608 assumption since additional scaling would be required, but the key properties of the model should remain
609 the same. Available experimental data from Lak et al. [14] does not particularly support any one of these
610 assumptions over the other, since neurons were recorded one at a time and each neuron was recorded
611 only over one block of trials. Simultaneous recording from multiple dopaminergic neurons that respond
612 to the same cue would be the most effective method. Any correlation between the deviations of activity
613 from their respective fitted functions would be strong evidence for the second assumption above.

614 All analyses in this study are based on two fundamental constraints. Firstly, the reward distributions
615 of all options always remain constant within each block, and the agent always has perfect knowledge of
616 when the contingency changes occur at block crossovers. When the task is generalised to a non-stationary
617 multi-armed bandit, the monotonic novelty representation by dopaminergic neurons is clearly no longer
618 optimal. An abrupt contingency change leads to a transient increase in the estimated reward variability
619 according to the learning rules of our model, and from a normative perspective, this is certainly as a marker
620 that could be used to trigger a reset or adjustment of the novelty representation. On the other hand, a
621 continuous graduate shift in the reward distribution would be more difficult to optimise for. The learning
622 rule with scaled reward prediction error proposed by Möller et al. [23] is beneficial when the spread of
623 the reward distribution (“noisiness” of the reward) is variable, but not when drastic changes in the mean
624 reward occur. It would be interesting to further investigate the learning dynamics and the resulting effect
625 on exploration modulation in these scenarios with this alternative learning rule, potentially also combined
626 with the dynamic learning rate we used in this study. Other models with variable learning rate such as
627 the adaptive learning rate models in Nassar et al. [42] and Diederer and Schultz [43] show significant
628 advantage in their adaptability in changing environments, which is an important complimenting feature
629 to our model.

630 Secondly, given the first constraint is satisfied, the agent should employ a stationary strategy in
631 respect of the trial number within a block. This could be violated when a situation with a known and
632 very limited number of trials are left before a contingency change, and there are still high uncertainty
633 levels associated with some of the actions. In such scenarios, exploratory behaviour could give way to
634 risk aversion. This is a possible but unlikely occurrence in the Gershman [12] experiments due to the

635 relatively small reward variability. Wilson et al. [3] investigated this phenomenon, but a mechanistic
636 model is yet to be developed. Since this mechanism would involve dynamics on a longer timescale, we
637 could potentially look for a shift in the tonic dopamine level as a contributor once the model is expanded
638 to account for its effect.

639 In conclusion, the model we propose in this work provides novel insights on how effective exploration
640 strategies could be achieved in the brain, specifically the basal ganglia, and generates interesting experi-
641 mental predictions. We expect future work to verify the new predictions and to further refine the model
642 for greater levels of detail and better generality.

643 4 Methods

644 4.1 Function fitting to neural recording data

645 The neural recording data used for function fitting is in the form of normalised and baseline-subtracted
646 average firing rate over the fixed-length temporal window after cue onset. Normalisation is performed by
647 dividing the raw firing rate during the measurement period by a reference firing rate taken immediately
648 before cue onset.

649 Three different functions were fitted to the novelty response of dopaminergic neurons. The inverse
650 square root function with two free parameters:

$$651 f(n) = m + \frac{k}{\sqrt{n}}. \quad (39)$$

652 The power function with three free parameters:

$$653 f(n) = m + kn^\pi. \quad (40)$$

654 The exponential function with three free parameters:

$$655 f(n) = m + ke^{\pi n}. \quad (41)$$

656 Two different techniques were used for model fitting. First, the average activity of all recorded neurons
657 at each given trial number was computed, and maximum likelihood fitting of three generative models
658 was done on the average activity using MATLAB function `fminsearch`. Bayesian information criterion
659 (BIC) statistics were then computed manually using the resulting maximum likelihood values. Second,
660 hierarchical mixed-effects models were fitted to individual neurons' recording data using MATLAB's
661 `nlmefit` function. BIC values were returned directly by the function. The population distribution of
662 model parameters were modelled both as a fully joint distribution and independent distributions of each

663 of the free parameters.

664 4.2 Model fitting to behavioural data

665 Eight different reinforcement learning strategies were fitted to behaviour of human participants. These
666 differ in two dimensions: learning rule and exploration type. Two learning rules and four exploration
667 types were tested, giving the total of eight models. One learning rule is derived from the basal ganglia
668 model and the other is the Kalman filtering as described in Gershman [12]. A full list of relevant equations
669 that define the strategies and the free parameters that were fitted to behaviour are listed in Table 1. Note
670 that the value utility function for random exploration (Thompson sampling) strategies with basal ganglia
671 model-derived learning rules is not nested within Equation 36 (since these strategies are not realistic
672 according to the results of our neural data analysis – they are included for completeness only). The value
673 utility for them is given by

674
$$T_i[t] = Q_i[t] + \lambda (((a + bm)Z)S_i[t] + bkZ\hat{\sigma}_i[t]). \quad (42)$$

675

676 The Kalman filter-based strategies used as a baseline and the methods used for fitting were described
677 in detail in Gershman [12]. Trial-by-trial model fitting of the strategies derived from the basal ganglia
678 model was done using MATLAB's `fmincon` function. Each individual participant were independently
679 fitted with a unique set of optimal parameters. Maximum likelihood fitting was used, with the choice
680 likelihood computed using the value utility function at each trial, and the sum-log-likelihood for each
681 individual participant maximised. The optimiser function was run repeatedly with 50 different initial
682 guesses, and the best results out of the repeated runs were taken. Initialisation of latent parameters
683 followed the same protocols of those used in Gershman [12].

684 4.3 Models used in simulation

685 We compared the performance of several different directed exploration (UCB) strategies in simulation
686 using more challenging bandit tasks. Specifically, we used a series of efficient deterministic strategies
687 detailed in Auer et al. [6] as well as the Kalman filter-based strategy [12] and neural-inspired strategies.
688 Here, the Kalman filter strategy and neural strategies were always initialised with mean reward and
689 standard deviation estimators all at 0.5 (which differs from the initialisation used in Gershman [12]
690 which assumes more knowledge about the task). Otherwise, the Kalman filter strategy follow the same
691 description given previously in Table 1, but with $e = 0$ to make the action selections deterministic (since
692 we are comparing here against other deterministic strategies). The free parameter θ was optimised for
693 each task. The neural strategies inspired by the basal ganglia model also largely follow the descriptions

Learning rule	Exploration type	Fixed parameters	Fitted parameters	Equations
Kalman filter	Hybrid	N/A	γ, θ	7
	Directed		θ, e	1
	Random		γ	4
	Value	$\theta = 0$	e	1
Basal ganglia (fixed LR)	Hybrid	$a = 1.380, b = 0.306, m = 0.677, k = 4.486, \pi = -0.791$	$\alpha_q, \alpha_s, \lambda, e$	15, 16, 17, 18, 19, 36
	Directed	$a = 0, b = 0, m = 0.677, k = 4.486, \pi = -0.791$	$\alpha_q, \alpha_s, \lambda, e$	
	Value	$a = 0, b = 0, m = 0, k = 0, \pi = 0, \alpha_s = 0$	α_q, e	
	Random	$a = 1.380, b = 0.306, m = 0.677, k = 4.486, \pi = -0.791, e = 0$	$\alpha_q, \alpha_s, \lambda$	15, 16, 17, 18, 19, 42

Table 1. Full description of strategies fitted to behavioural data. The fixed parameters are determined either by model constraints or neural recording data. The fitted parameters are the free parameters fitted to the behaviour of individual participants. Equations are the numbers of equations in previous text that describe the models. Note that for the Kalman filter models, the equations cited only describe the action selection but not learning through Kalman filtering. To see a full description of these models see Gershman [12].

given in Table 1, except all with fixed parameters $a = b = m = 0$. k then becomes a redundant parameter and is fixed to 1. Noise level e is also set to 0, same as for the Kalman filter strategy. π is set to either -0.5 (the value giving optimal reward posterior estimates) or -0.791 (the value obtained from experimental data). The remaining free model parameters α_q , α_s and λ were optimised for each of the tasks with a crude global minimisation search. In addition, we also fitted variations of the neural strategies with dynamically adjusted learning rates as described in Equations 37 and 38, in which cases the initial learning rate parameters $\alpha_{0,q}$ and $\alpha_{0,s}$ were optimised instead of α_q and α_s .

701 Acknowledgements

702 The Authors thank Moritz Moeller for discussion.

703 References

704 [1] Möller, M. and Bogacz, R. “Learning the payoffs and costs of actions”. *PLOS Computational Biology*
705 15.2 (2019), e1006285. DOI: [10.1371/journal.pcbi.1006285](https://doi.org/10.1371/journal.pcbi.1006285).

706 [2] Whittle, P. “Restless Bandits: Activity Allocation in a Changing World”. *Journal of Applied Prob-
707 ability* 25 (1988), pp. 287–298. DOI: [10.2307/3214163](https://doi.org/10.2307/3214163).

708 [3] Wilson, R. C., Geana, A., White, J. M., Ludvig, E. A., and Cohen, J. D. “Humans use directed and
709 random exploration to solve the explore-exploit dilemma”. *Journal of Experimental Psychology:
710 General* 143.6 (2014), pp. 2074–2081. DOI: [10.1037/a0038199](https://doi.org/10.1037/a0038199).

711 [4] Gittins, J. C. “Bandit Processes and Dynamic Allocation Indices”. *Journal of the Royal Statistical
712 Society: Series B (Methodological)* 41.2 (1979), pp. 148–164. DOI: [10.1111/j.2517-6161.1979.tb01068.x](https://doi.org/10.1111/j.2517-6161.1979.tb01068.x).

713 [5] Katehakis, M. N. and Veinott, A. F. “The Multi-Armed Bandit Problem: Decomposition and Com-
714 putation”. *Mathematics of Operations Research* 12.2 (1987), pp. 262–268. DOI: [10.1287/moor.12.2.262](https://doi.org/10.1287/moor.12.2.262).

715 [6] Auer, P., Cesa-Bianchi, N., and Fischer, P. “Finite-time Analysis of the Multiarmed Bandit Prob-
716 lem”. *Machine Learning* 47.2 (2002), pp. 235–256. DOI: [10.1023/A:1013689704352](https://doi.org/10.1023/A:1013689704352).

717 [7] Gittins, J., Glazebrook, K., and Weber, R. *Multi-armed Bandit Allocation Indices*. John Wiley &
718 Sons, 2011. 287 pp.

719 [8] Sutton, R. S. and Barto, A. G. *Reinforcement Learning, second edition: An Introduction*. MIT
720 Press, 2018. 549 pp.

721 [9] Robbins, H. “Some aspects of the sequential design of experiments”. *Bulletin of the American
722 Mathematical Society* 58.5 (1952), pp. 527–535. DOI: [10.1090/S0002-9904-1952-09620-8](https://doi.org/10.1090/S0002-9904-1952-09620-8).

723 [10] Lai, T. and Robbins, H. “Asymptotically efficient adaptive allocation rules”. *Advances in Applied
724 Mathematics* 6.1 (1985), pp. 4–22. DOI: [10.1016/0196-8858\(85\)90002-8](https://doi.org/10.1016/0196-8858(85)90002-8).

725 [11] Katehakis, M. N. and Robbins, H. “Sequential choice from several populations.” *Proceedings of the
726 National Academy of Sciences* 92.19 (1995), pp. 8584–8585. DOI: [10.1073/pnas.92.19.8584](https://doi.org/10.1073/pnas.92.19.8584).

727 [12] Gershman, S. J. “Deconstructing the human algorithms for exploration”. *Cognition* 173 (2018),
728 pp. 34–42. DOI: [10.1016/j.cognition.2017.12.014](https://doi.org/10.1016/j.cognition.2017.12.014).

729 [13] Mikhael, J. G. and Bogacz, R. “Learning Reward Uncertainty in the Basal Ganglia”. *PLOS Com-
730 putational Biology* 12.9 (2016), e1005062. DOI: [10.1371/journal.pcbi.1005062](https://doi.org/10.1371/journal.pcbi.1005062).

731 [14] Lak, A., Stauffer, W. R., and Schultz, W. “Dopamine neurons learn relative chosen value from
732 probabilistic rewards”. *eLife* 5 (2016). Ed. by M. J. Frank, e18044. DOI: [10.7554/eLife.18044](https://doi.org/10.7554/eLife.18044).

735 [15] Schultz, W. “Predictive reward signal of dopamine neurons”. *Journal of Neurophysiology* 80.1
736 (1998), pp. 1–27. DOI: 10.1152/jn.1998.80.1.1.

737 [16] Kakade, S. and Dayan, P. “Dopamine: generalization and bonuses”. *Neural Networks* 15.4 (2002),
738 pp. 549–559. DOI: 10.1016/S0893-6080(02)00048-5.

739 [17] Costa, V. D., Tran, V. L., Turchi, J., and Averbeck, B. B. “Dopamine Modulates Novelty Seeking
740 Behavior During Decision Making”. *Behavioral neuroscience* 128.5 (2014), pp. 556–566. DOI: 10.
741 1037/a0037128.

742 [18] Ljungberg, T., Apicella, P., and Schultz, W. “Responses of monkey dopamine neurons during learning
743 of behavioral reactions”. *Journal of Neurophysiology* 67.1 (1992), pp. 145–163. DOI: 10.1152/
744 jn.1992.67.1.145.

745 [19] Horvitz, J. C., Stewart, T., and Jacobs, B. L. “Burst activity of ventral tegmental dopamine neurons
746 is elicited by sensory stimuli in the awake cat”. *Brain Research* 759.2 (1997), pp. 251–258. DOI:
747 10.1016/S0006-8993(97)00265-5.

748 [20] Humphries, M., Khamassi, M., and Gurney, K. “Dopaminergic control of the exploration-exploitation
749 trade-off via the basal ganglia”. *Frontiers in Neuroscience* 6 (2012).

750 [21] Jaskir, A. and Frank, M. J. *On the normative advantages of dopamine and striatal opponency for
751 learning and choice*. 2022. DOI: 10.1101/2022.03.10.483879.

752 [22] Wilson, R. C. and Finkel, L. “A Neural Implementation of the Kalman Filter”. *Advances in Neural
753 Information Processing Systems*. Vol. 22. Curran Associates, Inc., 2009.

754 [23] Möller, M., Manohar, S., and Bogacz, R. “Uncertainty-guided learning with scaled prediction errors
755 in the basal ganglia”. *PLOS Computational Biology* 18.5 (2022), e1009816. DOI: 10.1371/journal.
756 pcbi.1009816.

757 [24] Chapelle, O. and Li, L. “An Empirical Evaluation of Thompson Sampling”. *Advances in Neural
758 Information Processing Systems*. Vol. 24. Curran Associates, Inc., 2011.

759 [25] Russo, D., Van Roy, B., Kazerouni, A., Osband, I., and Wen, Z. “A Tutorial on Thompson Sampling”.
760 *arXiv:1707.02038 [cs]* (2020). arXiv: 1707.02038.

761 [26] Thompson, W. R. “On the likelihood that one unknown probability exceeds another in view of the
762 evidence of two samples”. *Biometrika* 25.3 (1933), pp. 285–294. DOI: 10.1093/biomet/25.3-4.285.

763 [27] Moeller, M., Grohn, J., Manohar, S., and Bogacz, R. “An association between prediction errors and
764 risk-seeking: Theory and behavioral evidence”. *PLOS Computational Biology* 17.7 (2021), e1009213.
765 DOI: 10.1371/journal.pcbi.1009213.

766 [28] Dabney, W., Kurth-Nelson, Z., Uchida, N., Starkweather, C. K., Hassabis, D., Munos, R., and
767 Botvinick, M. “A distributional code for value in dopamine-based reinforcement learning”. *Nature*
768 577.7792 (2020), pp. 671–675. DOI: [10.1038/s41586-019-1924-6](https://doi.org/10.1038/s41586-019-1924-6).

769 [29] Thurley, K., Senn, W., and Lüscher, H.-R. “Dopamine Increases the Gain of the Input-Output
770 Response of Rat Prefrontal Pyramidal Neurons”. *Journal of Neurophysiology* 99.6 (2008), pp. 2985–
771 2997. DOI: [10.1152/jn.01098.2007](https://doi.org/10.1152/jn.01098.2007).

772 [30] Alcaro, A., Huber, R., and Panksepp, J. “Behavioral Functions of the Mesolimbic Dopaminergic
773 System: an Affective Neuroethological Perspective”. *Brain research reviews* 56.2 (2007), pp. 283–
774 321. DOI: [10.1016/j.brainresrev.2007.07.014](https://doi.org/10.1016/j.brainresrev.2007.07.014).

775 [31] Ikemoto, S. “Brain reward circuitry beyond the mesolimbic dopamine system: A neurobiological
776 theory”. *Neuroscience and biobehavioral reviews* 35.2 (2010), pp. 129–150. DOI: [10.1016/j.neubiorev.2010.02.001](https://doi.org/10.1016/j.neubiorev.2010.02.001).

777 [32] Schultz, W., Dayan, P., and Montague, P. R. “A Neural Substrate of Prediction and Reward”.
778 *Science* 275.5306 (1997), pp. 1593–1599. DOI: [10.1126/science.275.5306.1593](https://doi.org/10.1126/science.275.5306.1593).

780 [33] Berke, J. D. “What does dopamine mean?” *Nature Neuroscience* 21.6 (2018), pp. 787–793. DOI:
781 [10.1038/s41593-018-0152-y](https://doi.org/10.1038/s41593-018-0152-y).

782 [34] Morrens, J., Aydin, Ç., Janse van Rensburg, A., Esquivelzeta Rabell, J., and Haesler, S. “Cue-
783 Evoked Dopamine Promotes Conditioned Responding during Learning”. *Neuron* 106.1 (2020), 142–
784 153.e7. DOI: [10.1016/j.neuron.2020.01.012](https://doi.org/10.1016/j.neuron.2020.01.012).

785 [35] Kutlu, M. G., Zachry, J. E., Melugin, P. R., Tat, J., Cajigas, S., Isiktas, A. U., Patel, D. D.,
786 Siciliano, C. A., Schoenbaum, G., Sharpe, M. J., and Calipari, E. S. “Dopamine signaling in the
787 nucleus accumbens core mediates latent inhibition”. *Nature Neuroscience* (2022), pp. 1–11. DOI:
788 [10.1038/s41593-022-01126-1](https://doi.org/10.1038/s41593-022-01126-1).

789 [36] Gershman, S. J. and Tzovaras, B. G. “Dopaminergic genes are associated with both directed and
790 random exploration”. *Neuropsychologia* 120 (2018), pp. 97–104. DOI: [10.1016/j.neuropsychologia.2018.10.009](https://doi.org/10.1016/j.neuropsychologia.2018.10.009).

792 [37] Cieślak, P. E., Ahn, W.-Y., Bogacz, R., and Rodriguez Parkitna, J. “Selective Effects of the Loss
793 of NMDA or mGluR5 Receptors in the Reward System on Adaptive Decision-Making”. *eNeuro* 5.4
794 (2018), ENEURO.0331-18.2018. DOI: [10.1523/ENEURO.0331-18.2018](https://doi.org/10.1523/ENEURO.0331-18.2018).

795 [38] Adams, R. A., Moutoussis, M., Nour, M. M., Dahoun, T., Lewis, D., Illingworth, B., Veronese,
796 M., Mathys, C., Boer, L. de, Guitart-Masip, M., Friston, K. J., Howes, O. D., and Roiser, J. P.
797 “Variability in Action Selection Relates to Striatal Dopamine 2/3 Receptor Availability in Humans:
798 A PET Neuroimaging Study Using Reinforcement Learning and Active Inference Models”. *Cerebral
799 Cortex (New York, NY)* 30.6 (2020), pp. 3573–3589. DOI: [10.1093/cercor/bhz327](https://doi.org/10.1093/cercor/bhz327).

800 [39] Cinotti, F., Fresno, V., Aklil, N., Coutureau, E., Girard, B., Marchand, A. R., and Khamassi, M.
801 “Dopamine blockade impairs the exploration-exploitation trade-off in rats”. *Scientific Reports* 9.1
802 (2019), p. 6770. DOI: 10.1038/s41598-019-43245-z.

803 [40] Daw, N. D., O’Doherty, J. P., Dayan, P., Seymour, B., and Dolan, R. J. “Cortical substrates for ex-
804 ploratory decisions in humans”. *Nature* 441.7095 (2006), pp. 876–879. DOI: 10.1038/nature04766.

805 [41] Zajkowski, W. K., Kossut, M., and Wilson, R. C. “A causal role for right frontopolar cortex in
806 directed, but not random, exploration”. *eLife* 6 (2017). Ed. by M. J. Frank, e27430. DOI: 10.7554/
807 eLife.27430.

808 [42] Nassar, M. R., Wilson, R. C., Heasly, B., and Gold, J. I. “An Approximately Bayesian Delta-
809 Rule Model Explains the Dynamics of Belief Updating in a Changing Environment”. *Journal of*
810 *Neuroscience* 30.37 (2010), pp. 12366–12378. DOI: 10.1523/JNEUROSCI.0822-10.2010.

811 [43] Diederer, K. M. J. and Schultz, W. “Scaling prediction errors to reward variability benefits error-
812 driven learning in humans”. *Journal of Neurophysiology* 114.3 (2015), pp. 1628–1640. DOI: 10.
813 1152/jn.00483.2015.